A MEMS high-speed angular-position sensing system with RF wireless transmission

Winston Sun and Wen J. Li*
Center for Micro and Nano Systems, The Chinese University of Hong Kong

ABSTRACT

A novel surface-micromachined non-contact high-speed angular-position sensor with total surface area under 4mm^2 was developed using the Multi-User MEMS Processes (MUMPs) and integrated with a commercial RF transmitter at 433MHz carrier frequency for wireless signal detection. Currently, a 2.3 MHz internal clock of our data acquisition system and a sensor design with a 13μg seismic mass is sufficient to provide visual observation of a clear sinusoidal response wirelessly generated by the piezoresistive angular-position sensing system within speed range of 180 rpm to around 1000 rpm. Experimental results showed that the oscillation frequency and amplitude are related to the input angular frequency of the rotation disk and the tilt angle of the rotation axis, respectively. These important results could provide groundwork for MEMS researchers to estimate how gravity influences structural properties of MEMS devices under different circumstances.

Key words: non-contact rotation sensing, high-speed rotation sensing, micro rotation sensor, wireless micro sensor.

1 INTRODUCTION

Tachometers have been widely used to measure angular speeds of rotating objects. In general, contact mechanical-based tachometers are convenient but less accurate than AC or DC electromagnetic-based tachometers. According to Nachtigal [1] and Haslam et al. [2], each type has its own advantages and shortcomings depending on the applications. Generally, optical tachometers such as the one reported by Spooncer et al. [3] give relatively accurate readings with a wide rpm range. However, Kwa et al. [4] pointed out that some optical sensors are sensitive to background light and contamination. Recently, many new rotation-sensing devices have been developed based on different principles. Watanabe et al. [5] measured rotation speed from magnetized axes, Powell et al. [6] used magnetic sensors based on Faraday induction to measure rotation rate, and Fabian et al. [7] developed a capacitive sensor for angular motion detection. However, these techniques impose restrictions on the material properties or geometry of the rotational components to be measured, and all these sensors must be accompanied with a stationary reference, which is externally mounted to the systems' housing for proper operation. Many micro motion sensors have been fabricated and can be used for rotation sensing. Söderkvist [8], Madni et al. [9], and Voss et al. [10] also used piezoresistive, piezoelectric, and capacitive principles, respectively, but with applications mainly lower speeds (i.e., <1000rpm). We have developed a MEMS high-speed rotation sensor packaged with a commercial wireless-transmission system designed by Sun et al. [11, 12], all these sensors must be accompanied with a stationary reference, which is externally mounted to the systems' housing for proper operation. Our developed piezoresistive sensor is capable of wirelessly measuring rotation speeds with sensitivity of ~2Hz/rpm/V with 5V input in the 100 to 6000rpm rotation range. To the best of our knowledge, no one has reported successful integration of high-speed rotation sensors built using the CRONOS MUMPs commercial foundry service with wireless transmitted output before our work. In the current work, we have tested several structural and seismic mass designs for the above sensor to observe if the sensing system has enough sensitivity to detect gravitational effect if the system is rotated about an axis parallel to the ground. We have found that, for certain seismic mass and structural design combinations, the sensing system is capable of detecting gravitational force, and hence can be used simultaneously as a angular-position sensor. It is well known that, for surface-micromachined devices, gravity force is less important when compared to surface forces. However, for our sensor design and high-speed measurement range, centrifugal force will overcome surface forces, and hence, making the sensor angular-position sensitive. The result from the current work is reported in this paper.

* wen@acae.cuhk.edu.hk; phone +852 2609-8475; fax +852 2603-6002; http://www.acae.cuhk.edu.hk/~cmns, Rm. 413 MMW Building, CUHK, NT, Hong Kong SAR.

Smart Structure and Materials 2001: Smart Electronics and MEMS, Vijay K. Varadan, Editor,
Proceedings of SPIE Vol. 4334 (2001) © 2001 SPIE · 0277-786X/01/$15.00

2 MUMPS FABRICATED ROTATION SENSOR

2.1 CONCEPT AND DESIGN

The concept for measuring rotation speed of a spinning body using embedded micro-sensors is illustrated in Figure 1. A three dimensional illustration of the developed MCNC sensor is shown in Figure 2. Details of the MCNC layers and post-fabrication processes used were reported by Sun et al. [11]. Scanning electron microscope (SEM) picture of a pair of the surface-micromachined sensors is shown in Figure 3. The mass platforms are sacrificially released and are curved due to residual stresses between different thin film layers in this case. Three MUMPs thin film layers which make up the platforms are apparent in this picture: Poly 1, Poly 2, and Au. As shown in Figure 4, the platform of the reference sensor is not sacrificially released and can be used for temperature dependence adjustment of the sensing system.

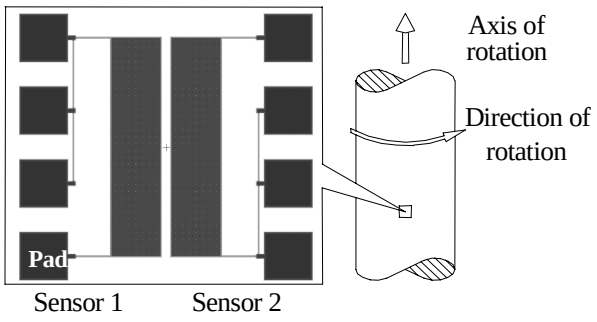

Figure 1. Conceptual drawing of micro sensors embedded in a rotating structure to measure rotation (not to scale).

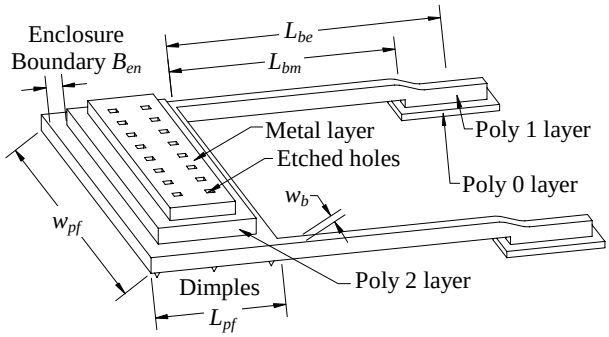

Figure 2. Three-dimensional drawing of a surface-micromachined rotation sensor using polysilicon as cantilever beams supporting a multi-layered mass platform.

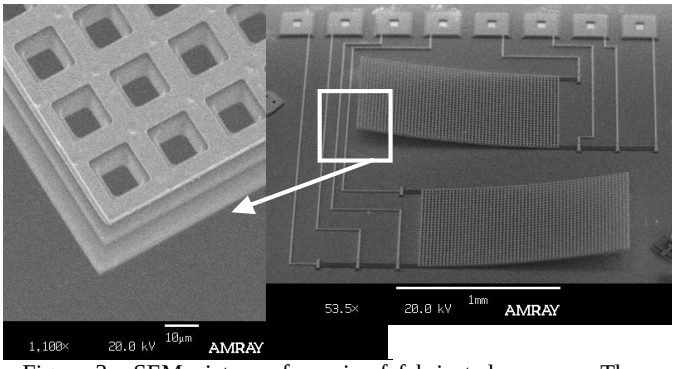

Figure 3. SEM picture of a pair of fabricated sensors. The MUMPs layers shown are Poly 1, Poly2, and Au.

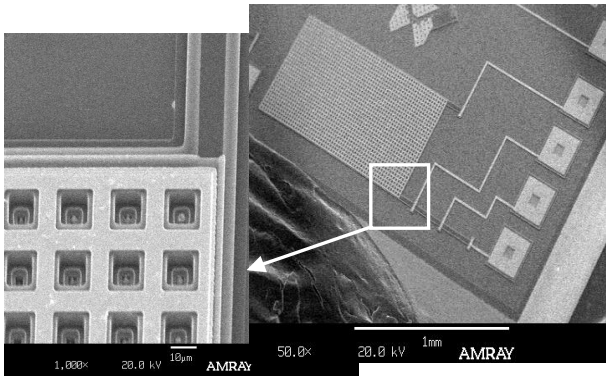

Figure 4. SEM picture of a reference sensor. MUMPs layers shown in the SEM include Poly 0, Poly 1, Poly 2, and Au.

2.2 THEORETICAL ANALYSIS

As shown in Figure 5, the initial horizontal moment arm measured from the centroid **c** to the fixed end **F** is just the beam length. At any non-zero angular velocity ω or angular acceleration α, such distance is reduced to a variable arm_{cg}. The vertical load $P = m \cdot r \cdot \omega^2$ induced by rotation and the axial load $N = m \cdot r \cdot \alpha$ caused by angular acceleration both act on the centroid **c** of the platform, where r is measured from the rotation axis to the neutral axis of the cantilever. The distance e_c is a constant measured from the platform to the neutral axis of the beam. The strain of a cantilever beam is maximum at **F**. From Fan et al. [11], the maximum allowable strain of polysilicon is about 1.7%. At $t > 0$ sec, the platform will be raised by a distance h_{cg} due to centrifugal force. Consequently, the stressed beams will be deflected in a curved shape and undergo slight elongation or shortening depending on the combined effect of P and N. The deflection or elongation of the beams causes a change of resistance of the polysilicon, which can be converted into a measurable change of voltage by arranging

the sensors in a Wheatstone-bridge configuration. The change of resistance due to beam elongation can be expressed as a function of gauge factor *G* as shown in the following equation:

$$\frac{\Delta R}{R} = G \cdot \varepsilon = G \cdot \frac{\Delta L}{L} \tag{1}$$

The approximate value for *G* is about 20 for polysilicon according to [14]. Typically sheet resistance for polysilicon is about 10 Ω/□ as given by Koester et al. [15]. When a steady state rotational speed is achieved, the axial load *N* tends to zero. The two sensors will have the same deflection and similar change of resistance. However, when α is >> 0, such as during motor startup or under sudden change of speed, the transient response of Sensor 1 and Sensor 2 will be different due to the contribution from *N*. Hence, by monitoring the transient response of the sensors, the direction of acceleration can be determined.

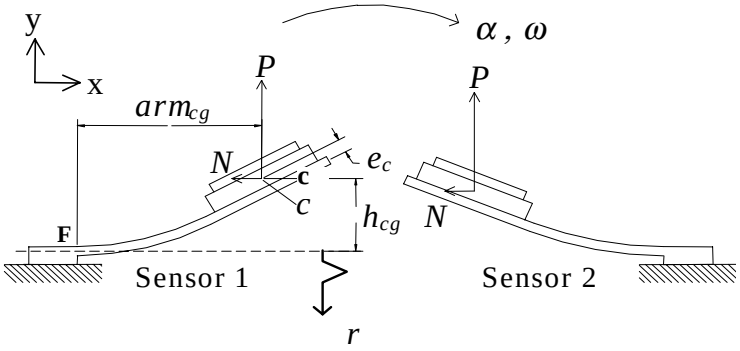

Figure 5. This illustration shows a pair of rotation sensors. The design parameters are also shown in this figure.

3 EXPERIMENTAL RESULTS

3.1 ANGULAR-SPEED SENSING

The conceptual drawing and a picture of the actual experimental setup to measure rotation speeds of a disk are shown in Figure 6. In our design, the rotating disk is replaceable. The power supply and the wireless transmission system chips are placed within a small package, which was made by a CNC plastic injection machine, and then placed on the rotating disk.

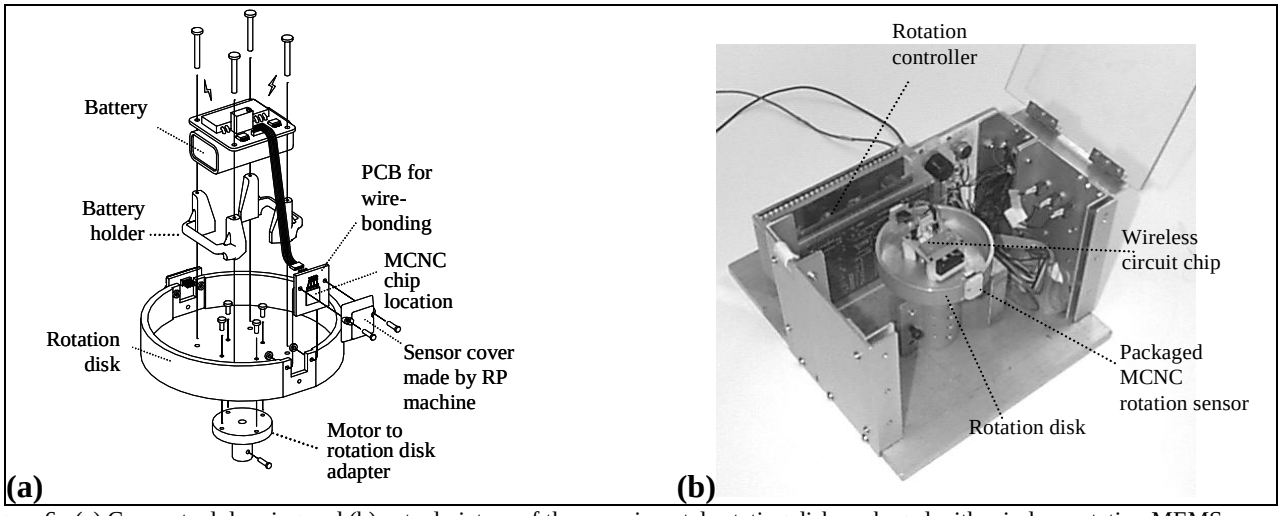

Figure 6. (a) Conceptual drawing and (b) actual picture of the experimental rotating disk packaged with wireless rotation MEMS sensor.

The MCNC fabricated sensors were tested for piezoresistivity by using probes to lift the platforms while measuring changes in resistance across the beam-platform-beam connection (see Figure 2). The variations of resistance versus deflection angle of the platform from the substrate for several sensor designs were tested and were shown to be non-linear but very consistent. As predicted by theory, narrower beams give higher resistance change and are prone to structural failure at higher deflection angles. For instance, in width×length convention, 14×100μm beams will fail at ~60^o while 20×200 and 30×200μm beams will survive beyond deflections angles of ~80^o. The beams of the sensor are arranged in a Wheatstone bridge configuration. The bridge leads were connected via wirebonding to PCB pads, and eventually to the signal transmission circuitry. Typical trend of the frequency output as a function of angular speed is shown in Figure 7. The response of the sensor (Figure 7) is non-linear as predicted; since the supporting cantilever beams underwent large deflections over the dynamic range tested.

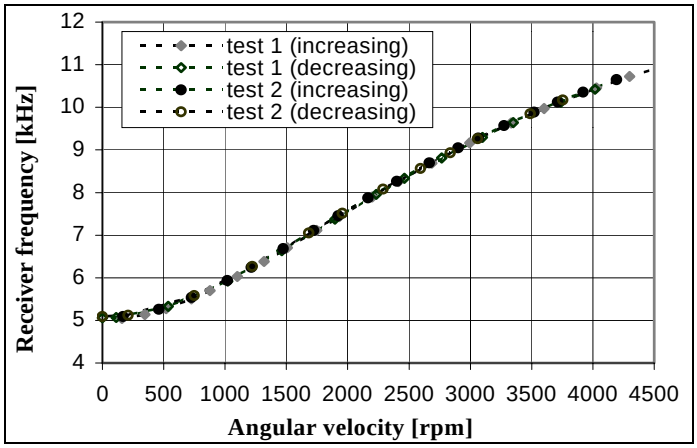

Figure 7. Wireless transmitted data from a rotation sensor. The sensor has a 600μm×320μm platform supported by 30μm×200μm beams, and was rotated on a 5cm radius disk. Some sensors were tested up to 6000rpm before beam failure.

If $\Delta R/R$ from (1) is replaced with the experimental results from probe-lifting (Figure 8), the pseudo-model described by Sun et al. [11] predicts the experimental data closely. Hence, the received frequency can be concluded as rotation data from the micro sensor. The sensors were also subjected to vibration and temperature tests, and the results were given in [12]. The comparison between the experimental results, the linear-deflection theory, and the pseudo-model is shown in Figure 9. The theory under-predicts sensor output at lower rpms possibly due to two factors: 1) piezoresistive change of the mass platform and 2) aerodynamic lifting of the mass platform.

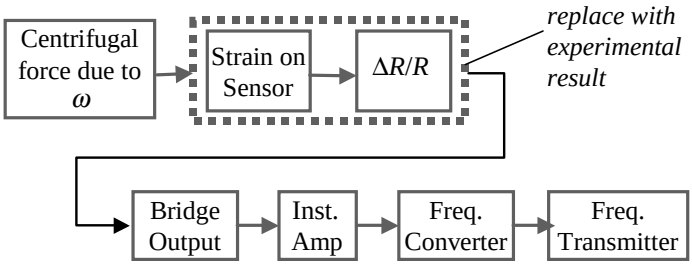

Figure 8. Schematic transfer function diagram of the sensor output frequency (Radiometrix receiver RX2 not shown) versus input ω through a series of intermediate steps including instrumentation amplifier AMP04, and frequency converter AD654, and the Radiometrix FM transmitter TX2. In the pseudo-model, $\Delta R/R$ is replaced with probe-lifting experimental data.

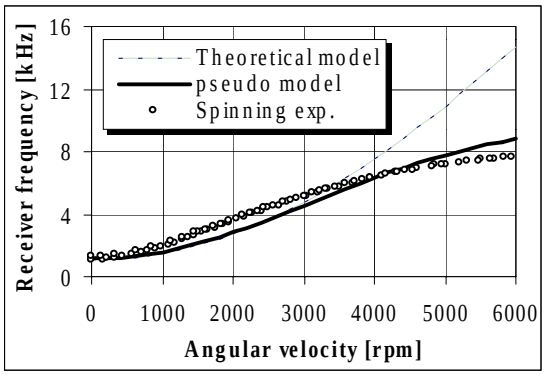

Figure 9. Comparison of experimental, theory, and theory plus lifting-experiment results.

3.2 ANGULAR-POSITION SENSING

We have oriented the entire experimental setup (Figure 6b) at different angles θ relative to the Z-axis as shown in Figure 10 and tested the effects of gravity on the sensor signal output. The wireless signal transmission system was found to have

enough sensitivity to measure fluctuations in sensor output due to gravity. For simplicity, if the aerodynamic forces are neglected, the total radial force F_r acting on the seismic mass as it rotates around a disk of radius r is:

$$F_r = m \cdot \left(r\omega^2 - g \sin(\theta) \sin(\phi) \right) \tag{2}$$

where m is the mass of the platform. This equation indicates that the gravitational effect can be neglected as long as r or ω is sufficiently large. However, if m is large enough, a sensing system may be able to detect F_r as a function of θ and ϕ, for some bounded values of r and ω. A plot of the ratio of gravitation force F_g and centrifugal force F_c on any given m is shown in Figure 11 for several disk radii (assuming θ=90° and ϕ =180°). For our sensing system, we are able to detect an F_g/F_c ratio of about 0.2% at 3000rpm on a 5cm radius disk. A data acquisition algorithm is employed to simultaneously acquire rotation speed signal from the optical encoder and frequency signal that is proportional to the angular-position and

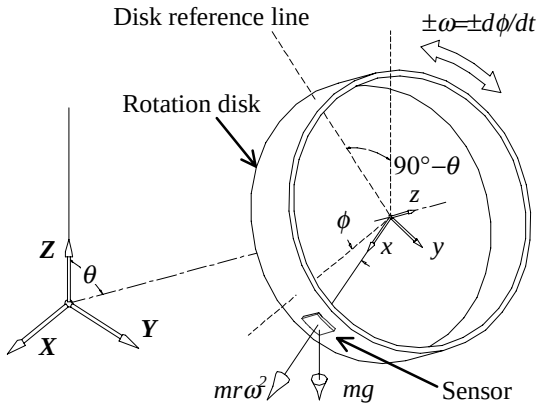

Figure 10. Conceptual drawing of the rotation setup showing definitions of θ, ϕ, and forces acting on the sensor.

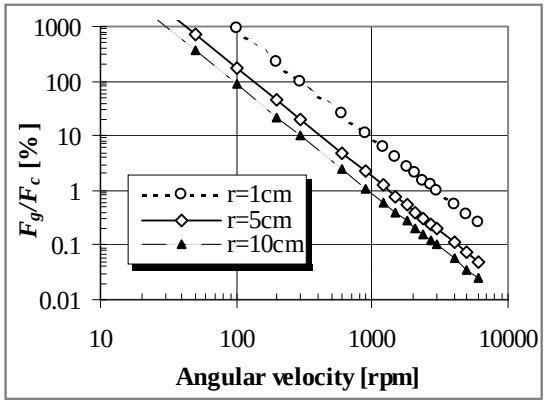

Figure 11. Variation of force in radial direction with respect to change in sensor angular position and tilt angle at 500rpm.

velocity from the receiver. This program is used to collect frequency signal data generated from the wireless rotation sensing system on a 5cm disk tilted at different θ. The results are presented below. As seen in Figure 12, the peak-to-peak variation at 300rpm and 0° tilt is less than 3Hz (frequency signal received by the receiver), which is less than 0.3% and considered negligible when compared to the nominal frequency around 1.06KHz. However, when the disk is tilted at 90°, a clear sinusoidal wave appears and the fluctuating amplitude is ~30Hz (Figure 13). This set of data is compared to the theoretical dependency of ϕ as given by (2) in the same figure, and it shows that the sinusoidal responses is indeed due to gravity. Hence, the angular position of the sensor on the disk can be obtained if the sampling frequency is sufficiently high and the output signal is calibrated. However, as shown in Figure 13, the sensor output is at 323.4rpm, which differs from

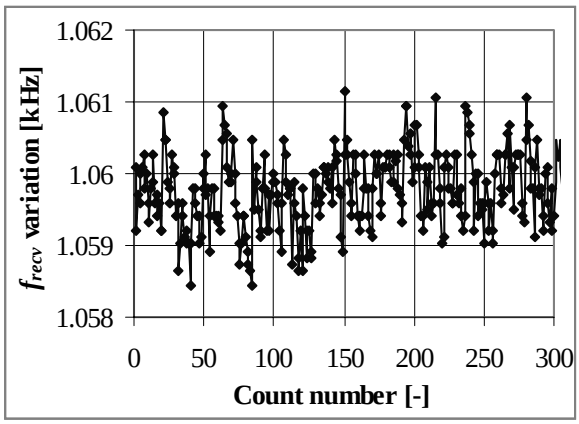

Figure 12. Receiver frequency variation of the sensor at 300rpm with 0° tilt.

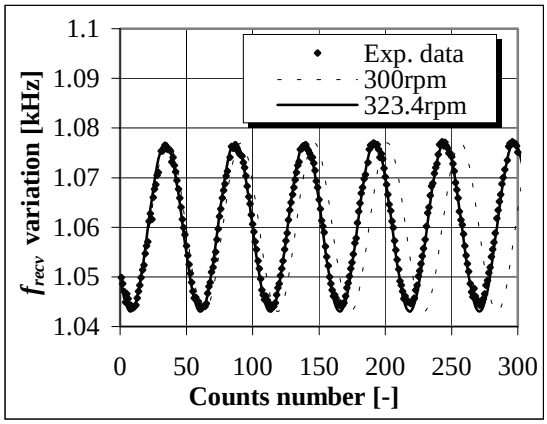

Figure 13. Receiver frequency variation of the sensor at 300rpm with 90° tilt. The experimental data is also compared to modeled data.

the optical encoder output of 300rpm. We have found that the difference is due to the mis-calibration of the optical encoder output, which illustrates an advantage of this gravity-dependent angular speed and position sensor: as along as the sensing system is able to give full peak-to-peak cyclical measurement, it does not need to be calibrated for receiver frequency drift. That is, ω and ϕ can be obtained from counting the cycles per unit time and measuring the instantaneous output amplitude, respectively.

We used Matlab's Power Spectrum Density (PSD) function to analyze the experimental data to estimate ω. The PSD for 300rpm at 0^o tilt signal is shown in Figure 14. Theoretically, if a sensor rotating at 300rpm has its output dependent on gravity, then the output signal should have spectrum peak at $f=\omega/60=5$Hz (the mass will undergo 1 cyclic vibration for every $\phi=360^o$). However, from Figure 14, the dominant peaks are below 0.2Hz and most likely due to the $1/f$ noise effect. The PSD of the same sensor tilted at 90^o is shown in Figure 15, which visibly shows a peak at 5.39Hz. The error is possibly due to the mis-calibration of the optical encoder, as discussed before. Nevertheless, this indicates that the dominant spectrum signal is due to dependence of the sensor on ϕ. This also indicates that obtaining the PSD can be an alternative method to read the rotation speed.

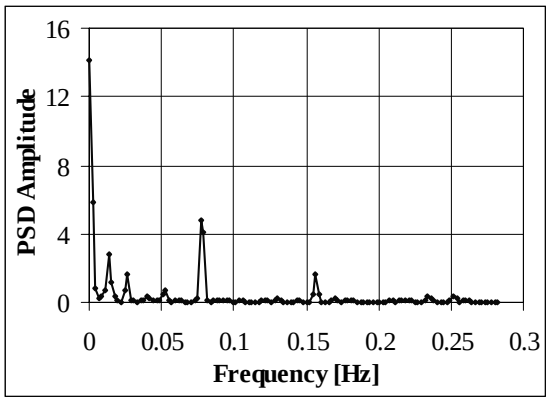

Figure 14. FFT spectrum showing peaks for a sensor tilted at 0° rotating at 300rpm.

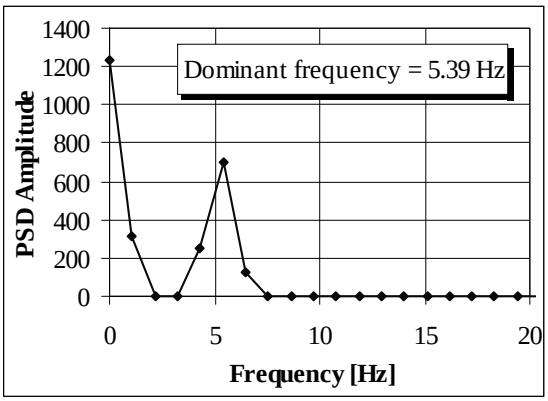

Figure 15. FFT spectrum showing peak at 5.39Hz for a sensor tilted at 90° rotating at 300rpm.

At rotation speed of 3000rpm with 90° tilt, the receiver frequency variation is shown in Figure 16. The sinusoidal waveform is not as obvious compared to that from 300rpm. However, as shown in Figure 17, the PSD peaks at 53.8Hz, corresponding to 3228rpm.

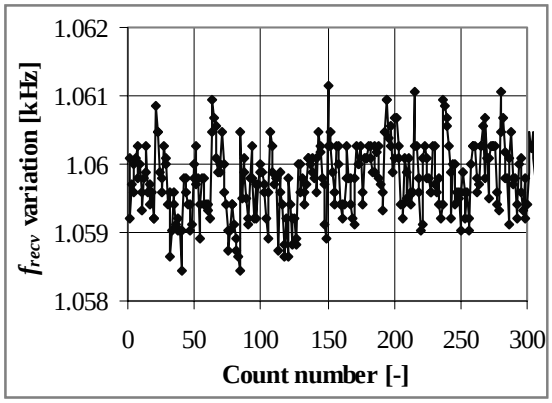

Figure 16. Time sequence signal of sensor rotating at 3000rpm with 90° tilt.

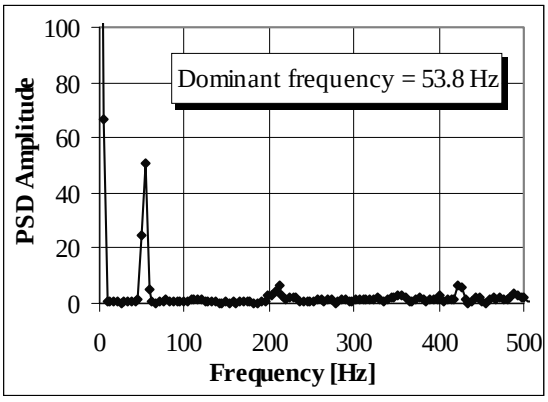

Figure 17. PSD of sensor rotation at 3000rpm with 90° tilt.

Experimental data were also obtained for the sensing system tilted and rotated at different θ and ω, respectively. Amplitude of the output signal variation is confirmed to be less at higher rotation speeds for any given tilt angle θ. The results at 300 and 1200rpm are shown in Figure 18. However, if the output is time averaged, the sensor output is independent of θ as shown in Figure 19. Hence, the sensing system can also be used to sense ω irrespective of θ.

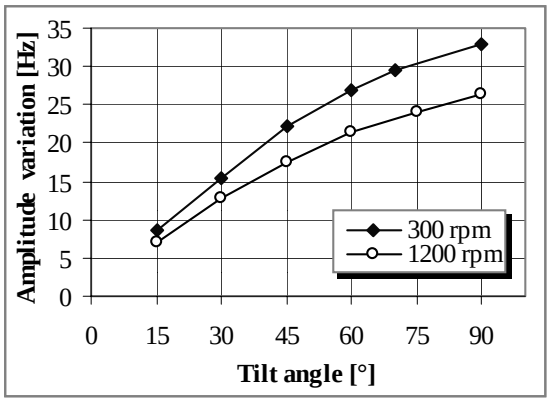

Figure 18. Variation of peak-to-peak amplitude of the receiver frequency at 300rpm and 1200rpm at different tilting angles.

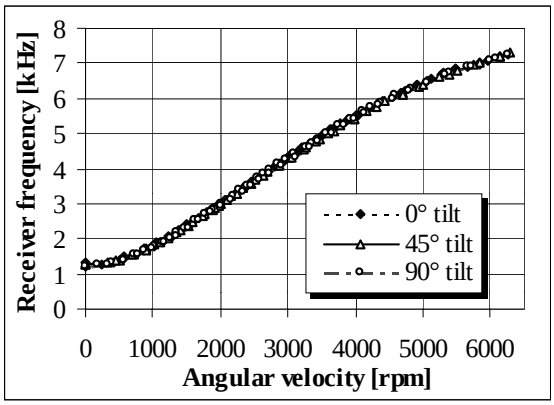

Figure 19. Orientation has insignificant effect on the overall trend of the receiver frequency response if the signal is averaged over time.

4 CONCLUSION

The design of a novel surface-micromachined rotation sensor for angular-position detection is presented. It is designed to detect the angular position of a rotating element by measuring the resistance change due to stress induced by centrifugal force on the seismic mass using piezoresistive effects. The designed sensors were fabricated using the MUMPs-29 run. A wireless transmission scheme for the rotation sensing system was evaluated, and the Radiometrix TX2 transmission chip gives stable and satisfactory performance. Experimental results showed a 13μg platform proof-mass could be used to detect rotation angle in the range of 180 rpm to around 1000 rpm at preferably over 30° non-vertical rotation axis. The sensing range can possibly be widened if a higher frequency internal oscillator of the data acquisition system is employed. We will further improve the sensing system by interfacing it with low-power wireless circuits and test the feasibility of using a pair of co-located structures for angular acceleration detection.

ACKNOWLEGMENTS

We would like to thank Mr. Martin Leung and Mr. Gary Lai for their help in data acquisition and spectrum analysis. This work was funded by the Chinese University of Hong Kong Research Direct Grant (2050173) and the Information Technology Entrepreneurs Program Grant (6900916).

REFERENCES

1. C. L. Nachtigal, *Instrumentation and Control – Fundamentals and Applications*, p. 370, New York, Chichester Wiley, 1990.
2. J. A. Haslam, G. R. Summers, and D. Williams, *Engineering instrumentation and control*, p. 133, London Edward Arnold, 1993.
3. R. C. Spooncer, A. S. Nicholson, and M. R. Oliver, "An optical tachometer with optical fibre links", *IEE Colloquium on IREM*, p. 1-3, 1991.
4. T. A. Kwa and R. F. Wolffenbuttel, "An integrated high-resolution optical angular displacement sensor", *IEEE Transducers '91*, p. 368-371, 1991.
5. K. Watanabe and C. Kim, "Non-contact revolution measurement by the magnetic field intensity from axes", *IEEE IMTC '94*, **2**, p. 605-608, 1994.
6. A. Powell and T. Meydan, "Optimisation of magnetic speed sensors", *IEEE Trans. on Mag. '96*, **32**, p. 4977-9, 1996.
7. T. Fabian and G. Brasseur, "A robust capacitive angular speed sensor", *IEEE IMTC '97*, **2**, p. 1267-1272, 1997.
8. J. Söderkvist, "Piezoelectric beams and angular rate sensors". *IEEE Proc. on the 44th Annual Symposium On Frequency Control*, p. 406-415, 1990.
9. A. M. Madni, L. A. Wan, and S. Hammons, "A microelectromechanical quartz rotational rate sensor for inertial applications", *IEEE Aeros. App. Conf.* **2**, p. 315-332, 1996.

10. R. Voss, K. Bauer, W. Ficker, T. Gleissner, W. Kupke, M. Rose, S. Sassen, J. Schalk, H. Seidel, and E. Stenzel, "Silicon angular rate sensor for automotive applications with piezoelectric drive and piezoresistive read-out", *IEEE Transducers '97*, **2**, p. 879-882, 1997.
11. W. Sun, T. Mei, W.-T. Ho, and W. J. Li, "A MEMS High-speed Rotation Measurement System with MCNC Fabricated Motion and Reference Sensors Using Wireless Transmission", *IEEE International Conference on Multisensor Fusion and Integration for Intelligent Systems*, Taipei, p. 226-231, 1999.
12. W. Sun, W.-T. Ho, W. J. Li, J. D. Mai, and T. Mei, "A Foundry Fabricated High-Speed Rotation Sensor Using Off-Chip RF Wireless Signal Transmission", *IEEE MEMS 2000*, p. 358-363, 2000.
13. L. S. Fan, Y. C. Tai, and R. S. Muller, "Integrated Movable Micromechanical Structures for Sensors and Actuators", *IEEE Trans. on Electron Devices*, **35**, p. 724-730, 1988.
14. V. Mosser, J. Suski, J. Goss, E. Obermeier, "Piezoresistive pressure sensor based on polycrystalline silicon", *Sensors and Actuators A (Physical)*, Lausanne, Switzerland, Elsevier Sequoia, **A28**, p. 113-132, 1991.
15. D. A. Koester, R. Mahadevan, B. Hardy, and K. W. Markus, *SmartMUMPS Design Handbook*, Rev. 4.0, MEMS Technology Applications Center, 1994.